FILE

INTERNAL DOCUMENT 211

I.O.S.

Results of the TOBI $\frac{1}{8}$ scale model wind tunnel tests

A.R. Packwood

May 1984

Internal Document No. 211

NATURAL ENVIRONMENT RESEARCH COUNCIL

INSTITUTE OF OCEANOGRAPHIC SCIENCES

INSTITUTE OF OCEANOGRAPHIC SCIENCES

Wormley, Godalming,
Surrey GU8 5UB
(042-879-4141)

(Director: Dr. A. S. Laughton, FRS)

Bidston Observatory,
Birkenhead,
Merseyside L43 7RA
(051-653-8633)
(Assistant Director: Dr. D. E. Cartwright)

Crossway,
Taunton,
Somerset TA1 2DW
(0823-86211)
(Assistant Director: M. J. Tucker)

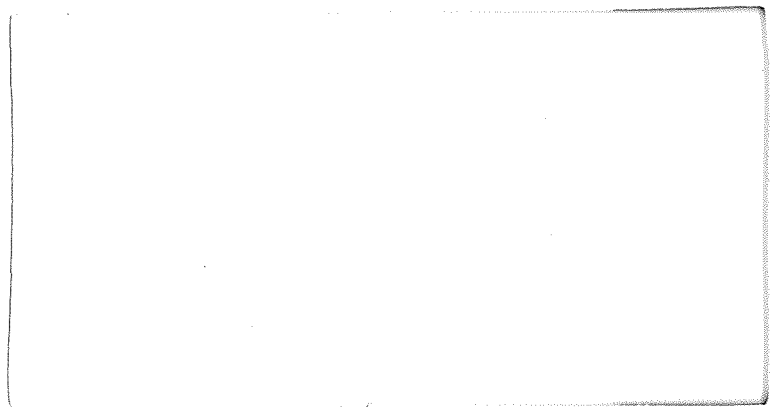

Results of the TOBI $\frac{1}{8}$ scale model wind tunnel tests

A.R. Packwood

May 1984

Internal Document No. 211

Institute of Oceanographic Sciences,
Brook Road,
Wormley,
Godalming,
Surrey,
GU8 5UB.

CONTENTS

RESULTS OF THE TOBI $\frac{1}{8}$ SCALE MODEL WIND TUNNEL TESTS

1. INTRODUCTION

TOBI is to be a deep towed ocean vehicle on which it is proposed to mount two 3 m long side-scan sonar arrays and a sub-bottom profiler, for surveying the deep ocean floor. The complete system will comprise an electro-mechanical tow cable attached to a depressor weight, which tows the instrument platform on a near neutrally buoyant umbilical cable of order 100 m in length. It is proposed that the instrument platform be slightly positively buoyant to reduce the risk of total loss. The proposed tow speed, when operating at full ocean depth, say 5 km or close thereto, will be limited to $\sim$ 1 m/s in order to keep the length of steel tow cable required within manageable limits.

In order to receive good signals from the isonofied sea bed, the instrument platform must remain in a stable attitude whilst being towed. The side-scan picture is badly degraded, in particular by yaw which should therefore be minimised. The purpose of the two body system is to minimise the motion of the instrument platform that would otherwise be induced by the heaving motion of the tow point on the ship if the main tow cable were connected directly to the instrument platform. Fig. 1 shows a predicted steady towing configuration indicating the desired crank angle in the cable at the depressor weight.

A scheme for the instrument platform that met the constraints imposed by the instrumentation and fell within the broad guidelines set for the hydrodynamic performance, as perceived, was drawn up by Roger Edge. A sketch of this is shown in fig. 2. The size of the depressor weight would depend upon the drag of this vehicle and since the vehicle's stability was of great operational importance, it was decided to undertake some model scale wind tunnel tests to determine these properties. A single tow point on a vertical centre line at the front of the vehicle had been decided upon for ease of terminating the umbilical, but its vertical location for trimming the vehicle also could not be determined without accurate model tests.

2. FLOW SIMILARITY LAWS AND CHOICE OF FACILITY

Since the vehicle is towed far below the free surface wave making or Froude similarity is unimportant. The flow and the hydrodynamic forces on the vehicle will therefore only be Reynolds number dependent. This means that for a reduced scale model the stability derivatives and force and moment coefficients can be more easily and cheaply determined in a wind tunnel than in a high speed water flume or tow tank. After investigating a number of facilities, the large wind tunnel at Bath University was found to be the only facility that could complete

the work in the given time schedule. The 5 ft x 7 ft aeronautical section of this tunnel has a maximum constant speed restriction of 40.5 m/s. A model scale of $\frac{1}{8}$ was chosen that was both suitable for the size of tunnel and convenient for fabrication. This gave a tunnel blockage ratio of $\sim$ 1% of the area. See fig. 3 for a description of the facility.

The main structure of the proposed vehicle will be fabricated in 5 cm diameter aluminium alloy tubes. In the ocean at a design tow speed of 1 m/s the Reynolds number (R_e) for flow around the tubes will be 3.1×10^4. For the $\frac{1}{8}$ scale model tested in air at say ISA sea-level conditions, the Reynolds number at maximum tunnel speed for flow around the tubes is only 1.74×10^4, which is equivalent to a full-scale speed of 0.56 m/s or 1.09 kn. The speed conversion factor under these conditions by Reynolds number scaling is $V_{model} = 72.2\ V_{full\text{-}scale}$. Fortunately in the R_e range $1.74 \times 10^4 < R_e < 3.1 \times 10^4$ the drag coefficient for flow around circular cylinders is almost independent of Reynolds number. However, when considering the Reynolds number for flow around the buoyancy spheres, the situation is not quite the same. In this case the Reynolds number range from model to prototype is $1.5 \times 10^5 < R_e < 2.7 \times 10^5$ which is in the trans-critical flow regime for the drag on a sphere where C_D is strongly dependent on R_e. Since the spheres are housed in ribbed hard-hats with an effective roughness ratio of 0.05, the flow can be expected to be fully separated. That being the case, the flow will again be largely independent of Reynolds number. Hence although operating at model scale at a lower Reynolds number than for the prototype, the conclusions, i.e. the non-dimensional force and moment coefficients, should be the same.

3. MODEL CONFIGURATIONS TESTED

From an early stage it was clear from the weight and buoyancy distribution of the vehicle that it would have good roll stability. Since in a wind-tunnel it would be impossible to model these static forces, it was decided that roll stability would not be investigated in the tunnel tests. Hence the model was tested in pitch and yaw configurations only. The balance on the Bath tunnel is a 3-component balance (lift, drag and pitching moment) so the model had to be turned on its side in order to make the measurements in yaw. The model was mounted on $\frac{1}{4}$" diameter rod between two vertical, streamlined balance arms 33 cm apart. The rod was clamped to the front of the model but was supported by ball-races in the balance arms and hence free to pivot. The rear of the model was supported on a tail wire via an extension bar. This wire was attached to a winch on the balance above the tunnel and passed through the floor of the tunnel to a weight suspended below. By this means the attitude of the model in the tunnel could be altered while the tunnel was in operation.

Since the vehicle is to be towed on a single cable, the position of the tow point becomes critical when trying to achieve a trimmed condition at zero incidence. For this reason the model was constructed with two clamping positions for the pitch axis in the plane of the proposed tow point. By interpolation, this would allow the vertical location of the tow point for the desired trim angle to be achieved.

Examination of the weight budget of the full-scale vehicle suggested that the 10 buoyancy spheres may not be sufficient to make the vehicle positively buoyant for the range of payload weights envisaged. To overcome this, high density syntactic foam buoyancy blocks were designed that would fit over the spheres. The requisite number of these could then be added to achieve the desired weight in water. Obviously a large number of configurations are possible but it would be very expensive to test them all. In order to cover the range of possibilities, it was decided to test two configurations, the first with no additional foam buoyancy and the second with a complete set of ten blocks, effectively covering all of the spheres in two boxes. This latter buoyancy distribution would give a 2.5 fold increase in the total buoyancy available. The model which was fabricated in wood, except for the spheres which were moulded in Araldite, is shown in these two configurations in figs. 4 and 5. For convenience these two configurations will be described as "lid on" with all the additional buoyancy blocks and "lid off" without. Fig. 6 shows the model mounted on its upper pitch axis in the wind tunnel. Note that the model is mounted upside-down, this is the traditional method for testing aeronautical models. Fig. 7 shows an end view looking down the tunnel towards the diffuser and fan.

The model was tested in the tunnel at an airspeed of 40.5 m/s at atmospheric pressure over incidence and yaw angle ranges of $\pm$ 10^{o} by 2^{o} steps in each of the configurations discussed above.

4. DISCUSSION OF RESULTS

Great care had to be taken in measuring the tare loads both "wind-off" static loads and "wind-on" loads on the balance arms and tail wire. This was because the aerodynamic lift and drag forces were found to be very small which meant that the tare forces were a significant fraction of the total measured force. For instance the drag tare was approximately one third of the total reading. All of the forces and moments measured were non-dimensionalized in the usual aeronautical fashion so that:

$$(C_D,\ C_L,\ C_Y) = \frac{(D,\ L,\ Y)}{qS}$$

$$(C_M,\ C_N) = \frac{(M,\ N)}{qSL}$$

where D, L, Y = drag, lift and side forces, M, N = pitching and yawing moments measured from the pitch and yaw axes at the front of the model, $q = \frac{1}{2}\rho V^2$ where ρ is the fluid density and V the undisturbed upstream velocity, and S is a representative area, taken to be S = L x W where L = 392.5 mm and W = 157.5 mm at model scale.

In order to test the assumption that at the tunnel velocity of 40.5 m/s the flow should be fully separated and Reynolds number independent, as discussed in section 2, the drag force was measured over a range of velocities from 18 - 41 m/s. The results, shown in fig. 8, indicate that in both configurations the drag becomes constant for wind speeds greater than 36 m/s. The implication is that the aerodynamic coefficients will be constant at speeds greater than this, which is equivalent to a full scale tow speed of 0.97 kn, and therefore will be representative of full scale towing conditions in the anticipated speed range of 1 to 2 kn.

4.1 LONGITUDINAL TESTS

Fig. 9 shows the variation of lift with incidence at zero yaw angle for the two configurations mounted on both upper and lower pitch axes. Within the accuracy of the measurements the results for upper and lower axes agree, as one would expect. The lift curve slopes are significantly different lid on and lid off, being about 53% higher in the lid on case. It is important to note that the vehicle generates small positive lift at zero incidence in both configurations. In the lid off case, the lift is equivalent to approximately 4 kgf at 1 m/s full-scale, and about twice this in the lid on case. The trim angle for zero lift is between 2^o and 3^o nose down.

Fig. 10 gives the drag variation with incidence. At zero incidence there is very little difference in drag between the two configurations and the variation over $\pm 10^o$ only changes from the minimum by about 20%. If the minimum lid off drag coefficient is converted to one based upon the frontal area within the front frame (~ 0.965 m^2 full scale) then the drag coefficient becomes 1.33. In full scale dimensional units this drag is equivalent to a force of $D \simeq 67\ V^2$ kgf where V is in m/s.

Figs 11 and 12 give some of the most significant and valuable results of the test series. By linearly interpolating between the upper and lower axes lines on fig. 11 to the zero pitching moment point on the zero incidence ordinate, then the optimum vertical position for the tow point giving

$C_M = 0$ at $\alpha = 0$ can be determined for the two configurations.

Relative to the top datum, shown in the sketch, the optimum tow point location is then given by y = 51.4 mm lid off and y = 32.2 mm lid on, or at full scale y = 407 mm lid off and y = 256 mm lid on.

By carrying out the same calculation for incidences of $\pm 2^o$ it is possible to determine the sensitivity of trim angle to variations in the vertical location of the tow point. Over this range the variation is close to being linear and in the lid off case gives a sensitivity of $\Delta y \simeq 51$ mm per degree change of trim at full scale and for the lid on case $\Delta y \simeq 64$ mm per degree. This means that a vertical movement of the tow point by the increment Δy will result in a 1^o change in trim angle. In each case moving down will result in a more nose up trim angle in pitch and vice versa.

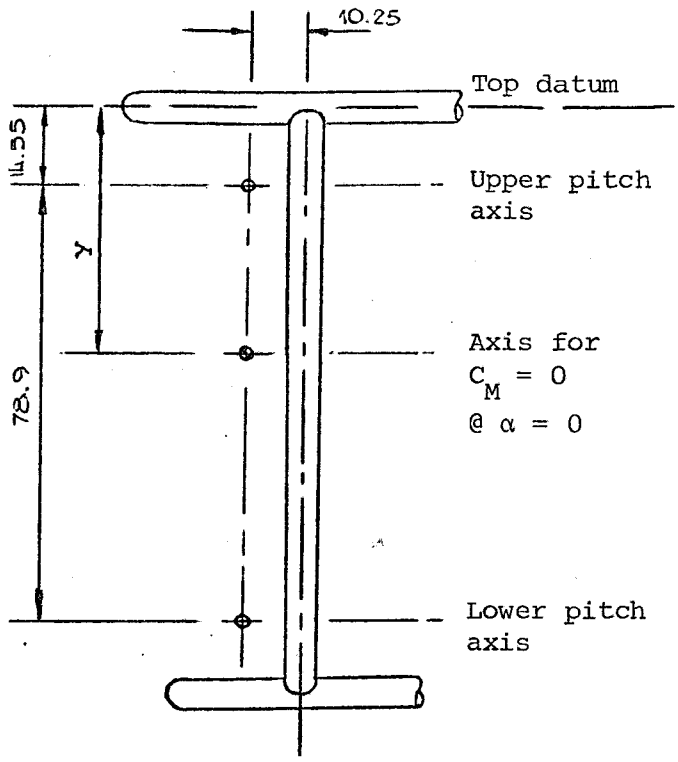

Model-scale dimensions (mm)

The distance, x_{ac} of the aerodynamic centre aft of the pitch axis gives a measure of the longitudinal pitch stability of the vehicle. The position of the aero. centre, which is the point about which the pitching moment, C_{Mac}, is constant with lift, can be derived from the pitching moment equation (see Houghton & Brock (1972))

$$C_M = C_{Mac} - \frac{x_{ac}}{L} (C_L \cos \alpha + C_D \sin \alpha)$$

Differentiating with respect to C_L and assuming α small gives

$$\frac{\partial C_M}{\partial C_L} = -\frac{x_{ac}}{L} \left(1 + \frac{\partial (C_D \alpha)}{\partial C_L}\right)$$

$$= -\frac{x_{ac}}{L} \left\{1 + \alpha \frac{\partial C_D}{\partial C_L} + C_D \frac{\partial \alpha}{\partial C_L}\right\} \quad \text{... since } \frac{\partial C_{Mac}}{\partial C_L} = 0 \text{ by definition}$$

The second term in the brackets is small since α is assumed small and as already noted C_D does not vary very much with α or C_L, so ignoring this term gives

$$\frac{x_{ac}}{L} = -\frac{\partial C_M}{\partial C_L}\left\{1 + C_D \frac{\partial \alpha}{\partial C_L}\right\}^{-1}$$

Averaging the slopes of the upper and lower axis curves in fig. 12 for each configuration gives

$$\frac{\partial C_M}{\partial C_L} = -0.63 \text{ lid off; } -0.51 \text{ lid on.}$$

Combining this data with the drag and lift curve slope information already obtained yeilds

$$\frac{x_{ac}}{L} = 0.40 \text{ lid off; } 0.37 \text{ lid on.}$$

These results are significantly larger than the usually quoted figures of 23 - 25% for low drag, high lift wing sections, which indicates greater longitudinal pitch stability.

4.2 LATERAL TESTS

The lateral force and moment characteristics, at zero incidence and a range of yaw angles $-10^\circ \leqslant \psi \leqslant +10^\circ$ shown in figures 13 - 16, show a similar pattern to the results of the longitudinal tests contained in figs 9 - 12. Since the vehicle is symmetrical in the plane of its vertical centre-line, only one central yaw axis at the front of the vehicle was used. Figs 13 and 14 show the side-force and drag variations with yaw angle. To within measurement accuracy these curves are symmetrical about $\psi = 0$ and the differences lid on and lid off are smaller than in the longitudinal tests. Fig. 14 gives a useful check on the drag coefficient at $\alpha = \psi = 0$ which is within 3° of that shown in fig. 10. This difference may be due to the different shielding of the tail wire by the model in the different mounting arrangements.

The yawing moment measurements are shown in figs 15 and 16. The fact that neither the side force, C_Y, or the yawing moment, C_N, curves pass through the origin, as would be expected for a symmetrical body, may in part be due to measurement errors which in general were 0 (1%) or, more probably, due to a pitch error in the free-stream at the centre-line of approximately 0.5° in the aeronautical working section. This had been measured by earlier workers during the tunnel calibration. The speed holding was very good, generally better than $\pm$ 0.2%.

From the results of figs 13 and 16 it is possible to deduce the approximate location of the lateral aerodynamic centre, $\bar{x}_{ac}$, relative to the yaw axis.

By a similar argument to that used to calculate x_{ac} we find

$$\frac{\bar{x}_{ac}}{L} = - \frac{\partial C_N}{\partial C_Y} \left\{ 1 + C_D \frac{\partial \psi}{\partial C_Y} \right\}^{-1}$$

from which

$$\frac{\bar{x}_{ac}}{L} = 0.45 \text{ lid off; } \quad 0.42 \text{ lid on}$$

5. CONCLUSIONS

On the whole the tunnel tests have proved of great benefit in providing valuable data that will assist in the design of the other components in the scheme and give understanding to the complex possible behaviour of the two body towed system. The results have allayed fears that the instrument platform, fabricated as it is in the form of a tubular "bed-stead", might have proved unstable. For it can be concluded that the present vehicle has very good stability, in fact more than might have been expected for a streamlined shape.

The tests have also predicted some useful points that would not have been foreseen. The present configurations generate a small amount of lift at zero incidence that will have to be allowed for in calculating the overall configuration of the system. The "lid on" configuration gives about twice as much lift as the "lid off" case. The drag of the vehicle is approximately 67 kgf at a tow speed of 1 m/s which is 16 times the "lid off" lift at the same speed. The pitching moment curves have shown that, despite the lift force, the vehicle can still be trimmed to tow at zero incidence by adjusting the height of the tow point. This position changes by about 150 mm in the case of the two configurations tested. It would seem sensible therefore to allow for a range of tow point locations between 200 mm and 450 mm below the top horizontal datum at a pitch of 50 mm, see fig. 17. A 50 mm change in the height of the tow point results in about a 1^{o} change in trim angle.

The stability calculations indicate that in both pitch and yaw the "lid off" configuration is the more stable of the two. It seems unlikely that all of the buoyancy blocks, represented in the lid on configuration, will be required. Current payload estimates suggest that perhaps four blocks may be sufficient. The mounting of four blocks will increase the drag slightly above the lid off measurements but they are unlikely to significantly influence the stability of the vehicle. It is felt that the two configurations tested have bracketed the stability range for the presently envisaged vehicle. It is also very comforting to note that in both configurations the yaw stability is better than the pitch stability. On the whole therefore the results are very encouraging and vindicate the decision to go for a "bedstead" type instrument platform.

ACKNOWLEDGEMENTS

The author would like to acknowledge the work of Roger Edge in designing and laying out the scheme for the prototype and model, Harold Plato for fabricating the model with great skill and members of the instrument workshop for moulding the model spheres; also Drs Wingham and Henderson of Bath University for carrying out the tunnel tests and giving advice in interpreting the results.

REFERENCE

Houghton E.L. and Brock A.E. (1972). Aerodynamics for Engineering Students. pub. E. Arnold Ltd., London, pp. 458.

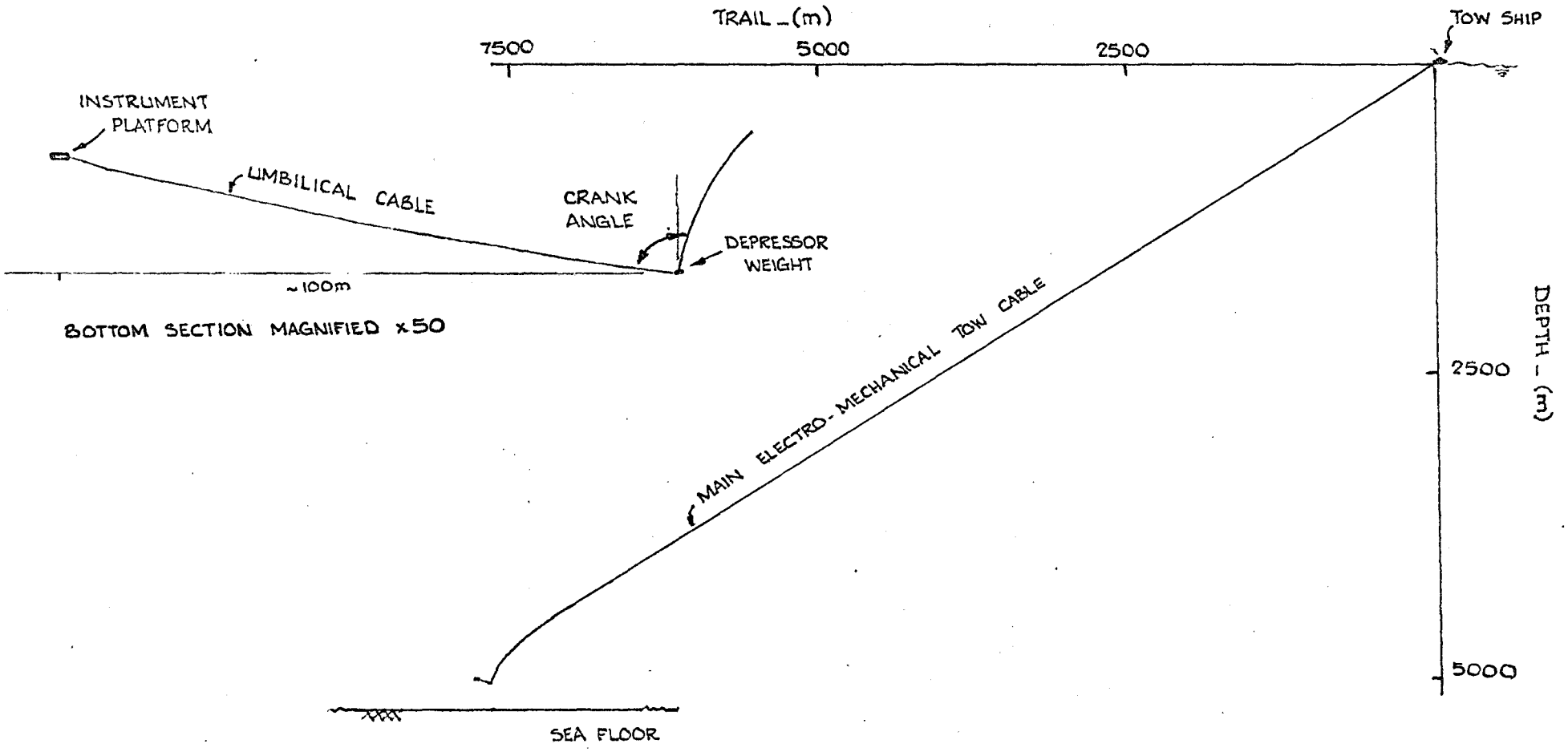

FIG. 1. PREDICTED STEADY STATE TOWING CONFIGURATION AT 1m/s ON 17mm CABLE

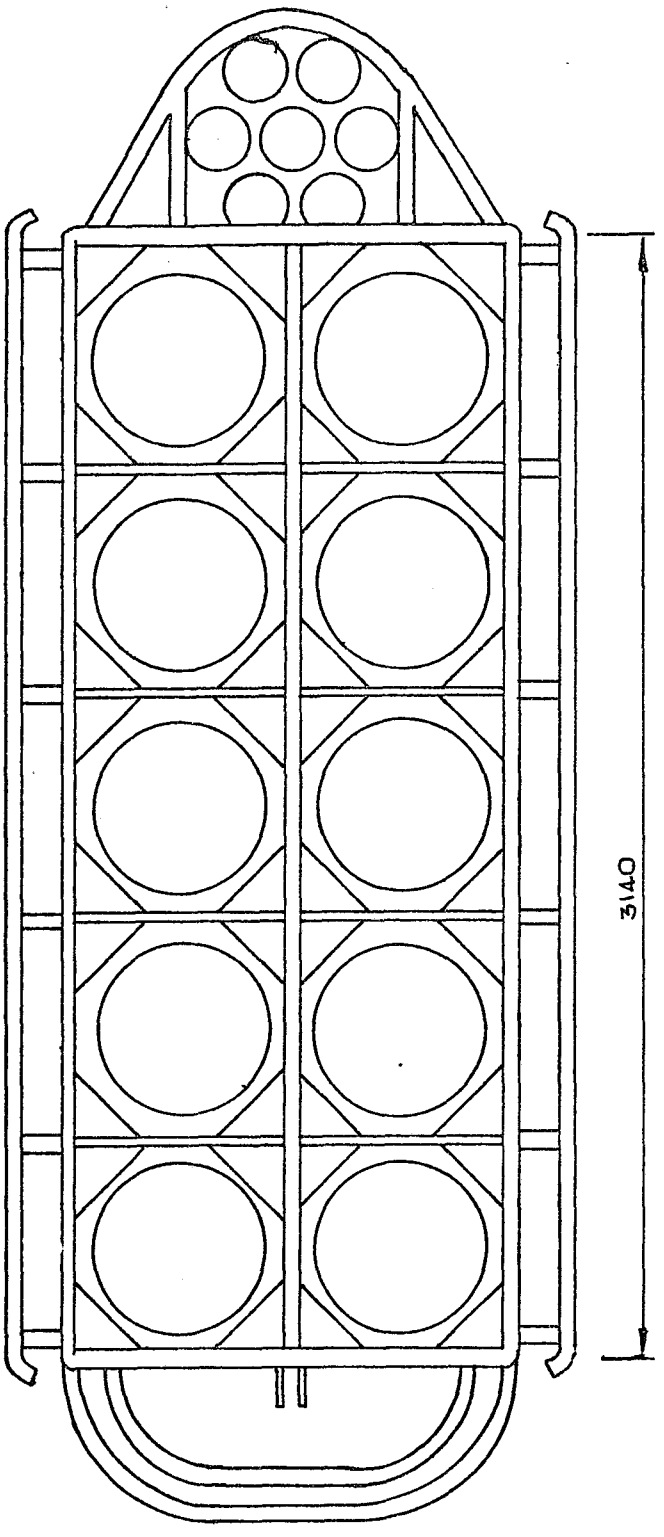

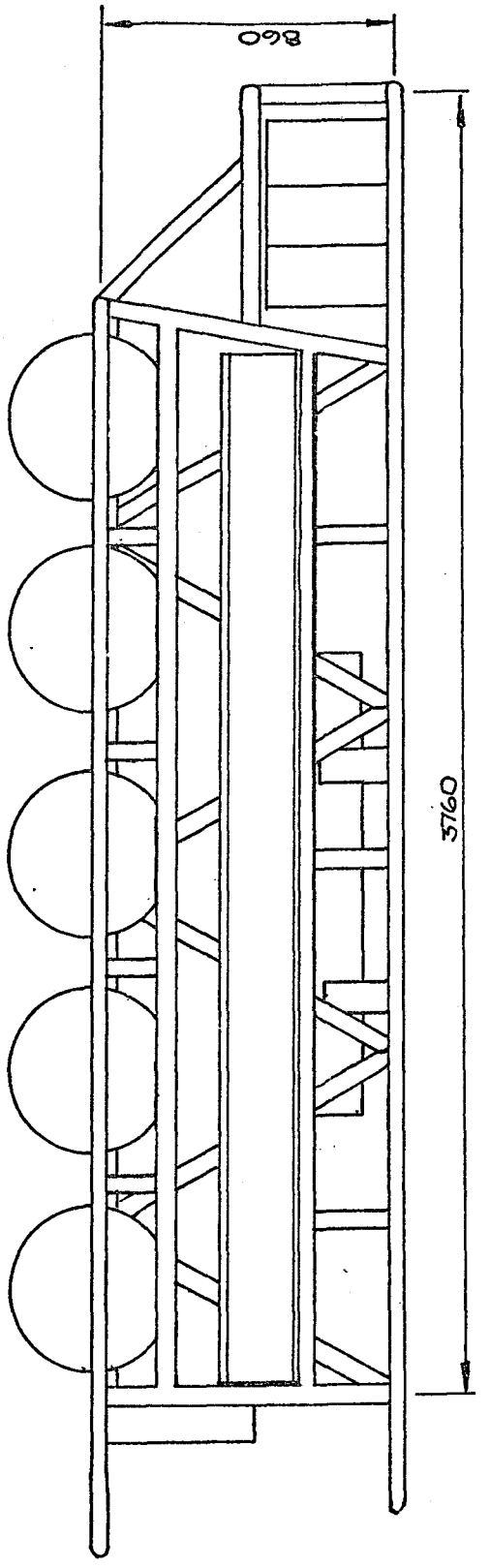

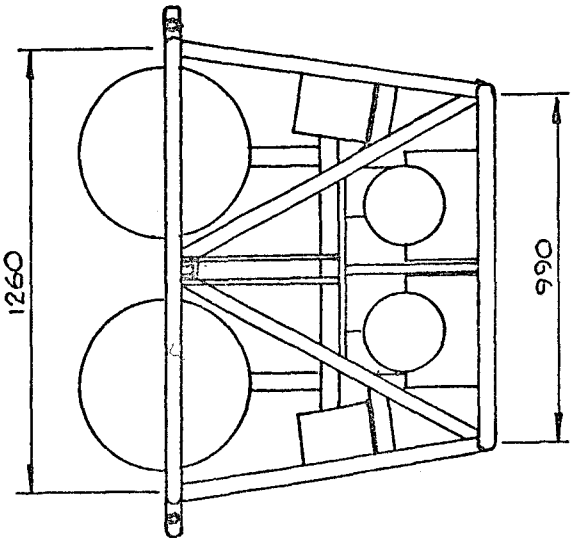

FIG. 2 SKETCH OF THE PROPOSED SCHEME FOR 'TOBI'

DIMENSIONS _ mm

BATH UNIVERSITY

LAYOUT OF LARGE DUAL PURPOSE WIND TUNNEL

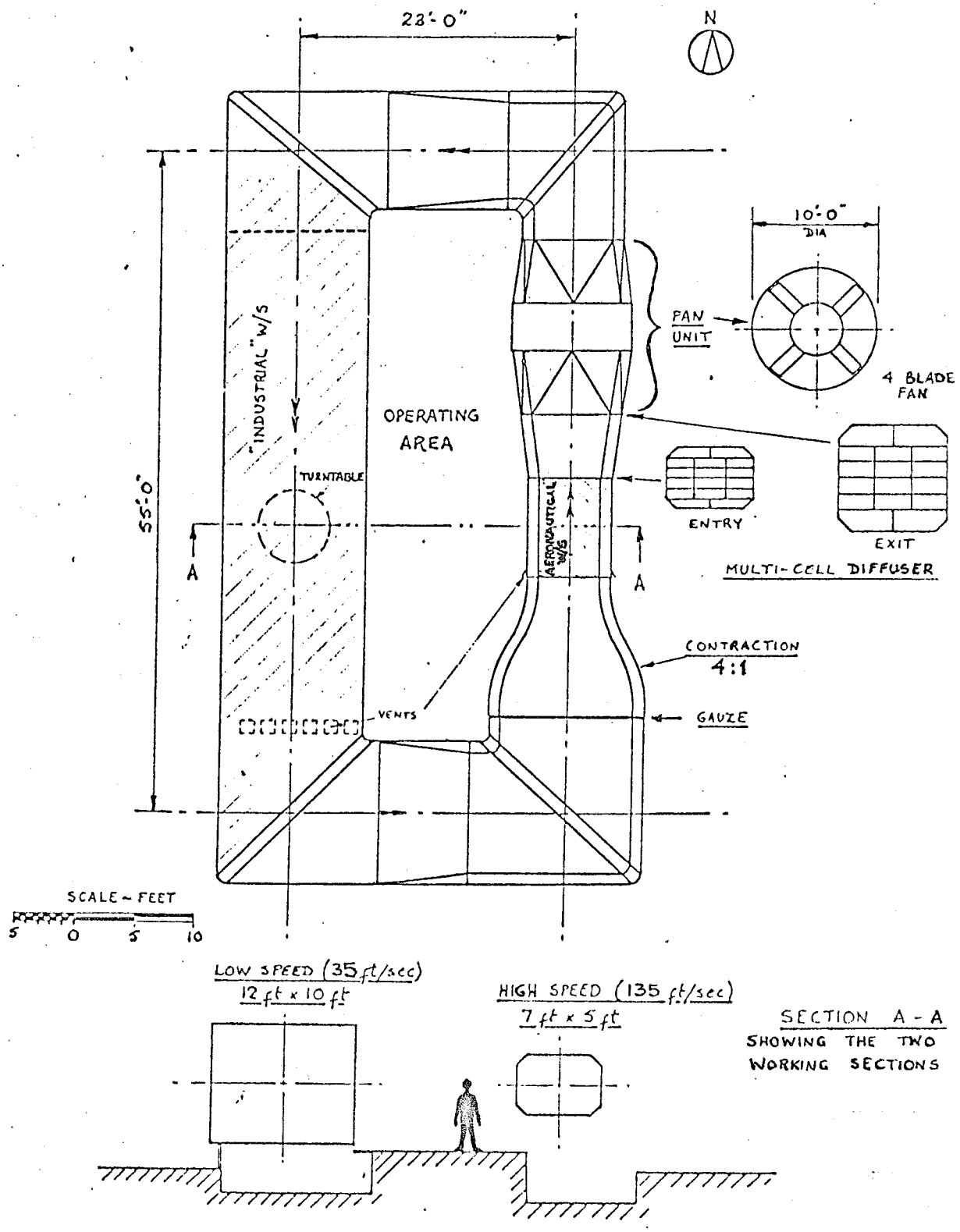

SECTION A - A
SHOWING THE TWO WORKING SECTIONS

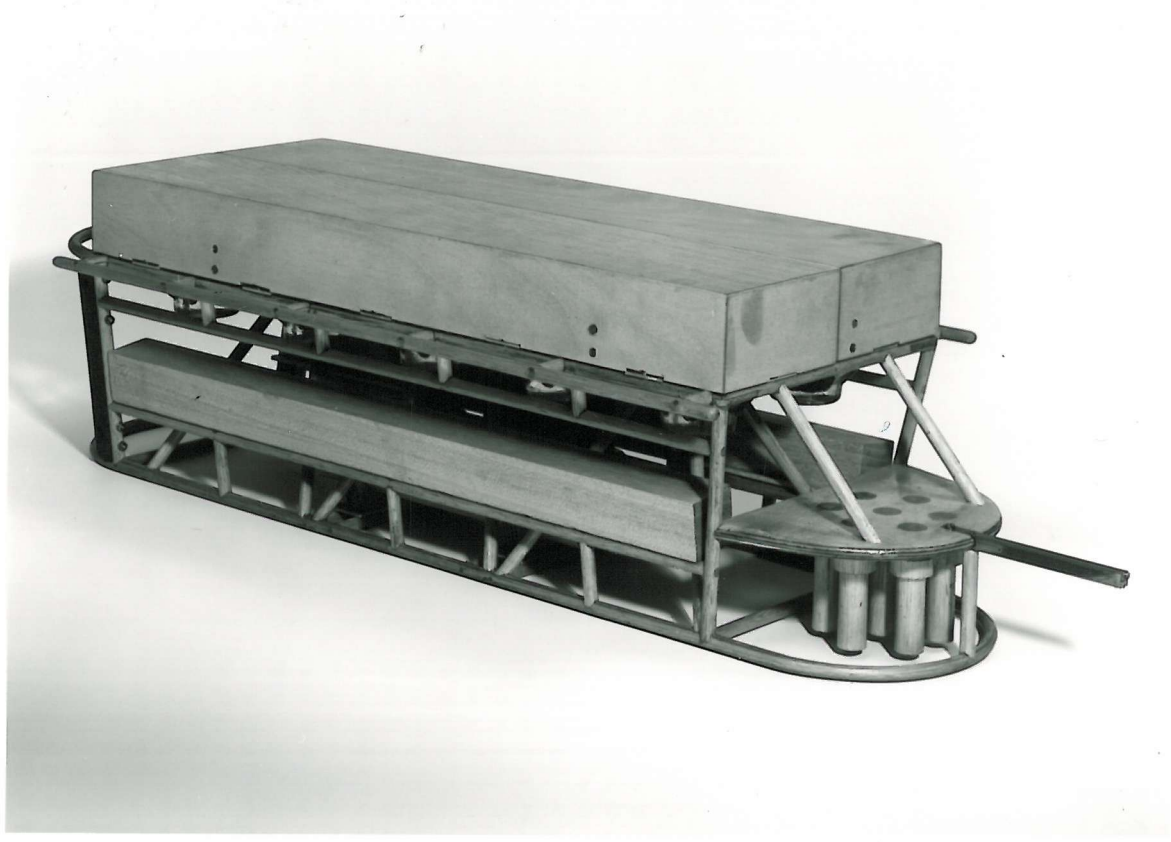

FIG. 4 $\frac{1}{8}$ scale model in "lid-on" configuration

FIG. 5 Model in "lid-off" configuration

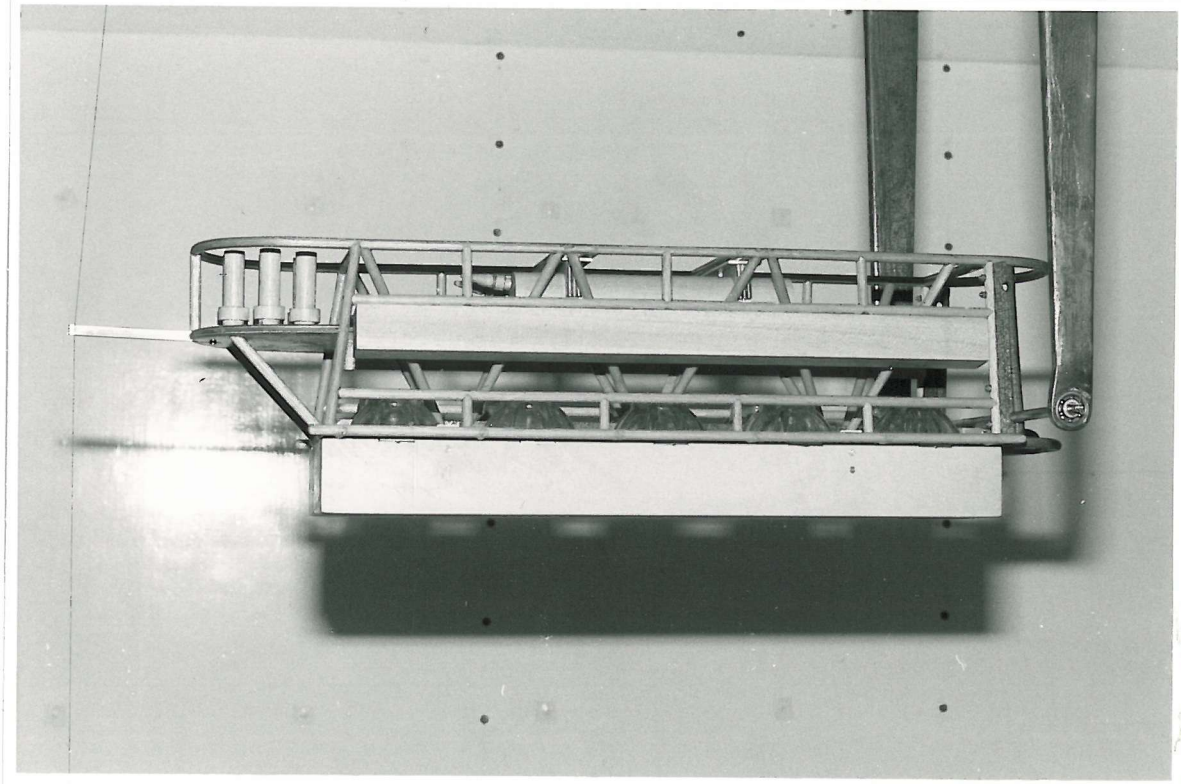

FIG. 6 Side view of the model mounted upside-down on its upper pitch axis in the wind tunnel

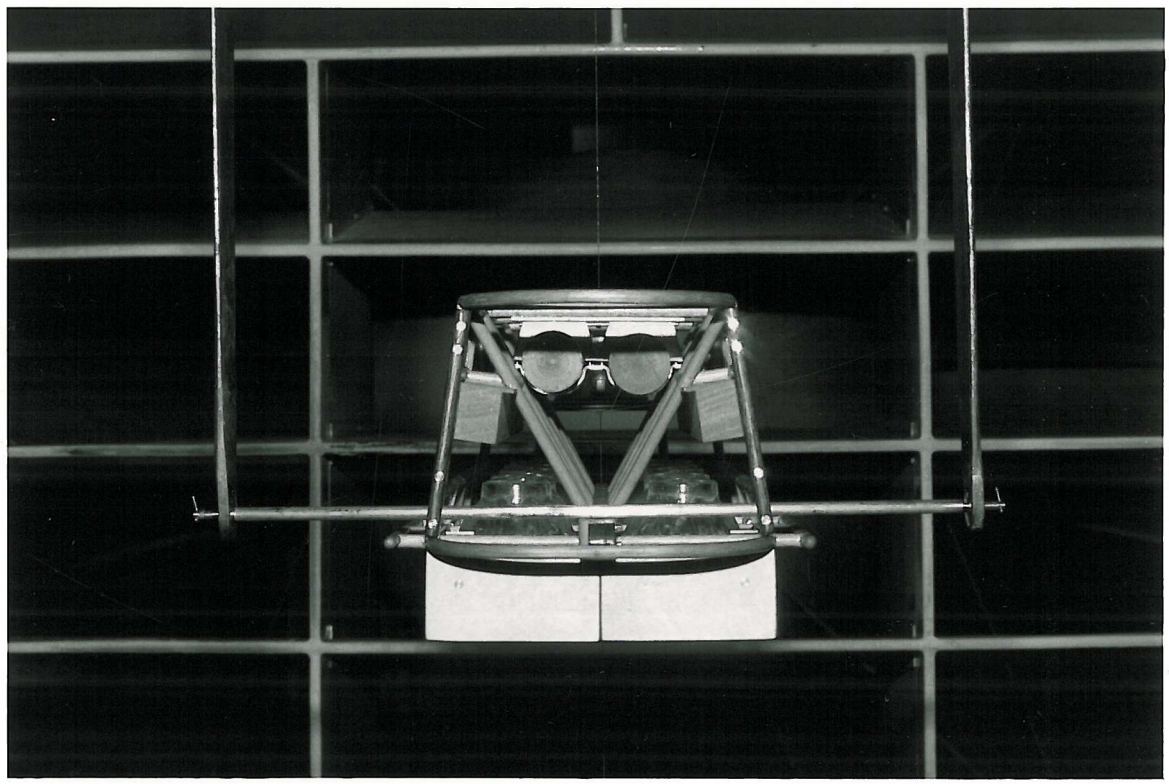

FIG. 7 Front view of the configuration shown in Fig. 6

Fig. 8

$C_D \sim V$

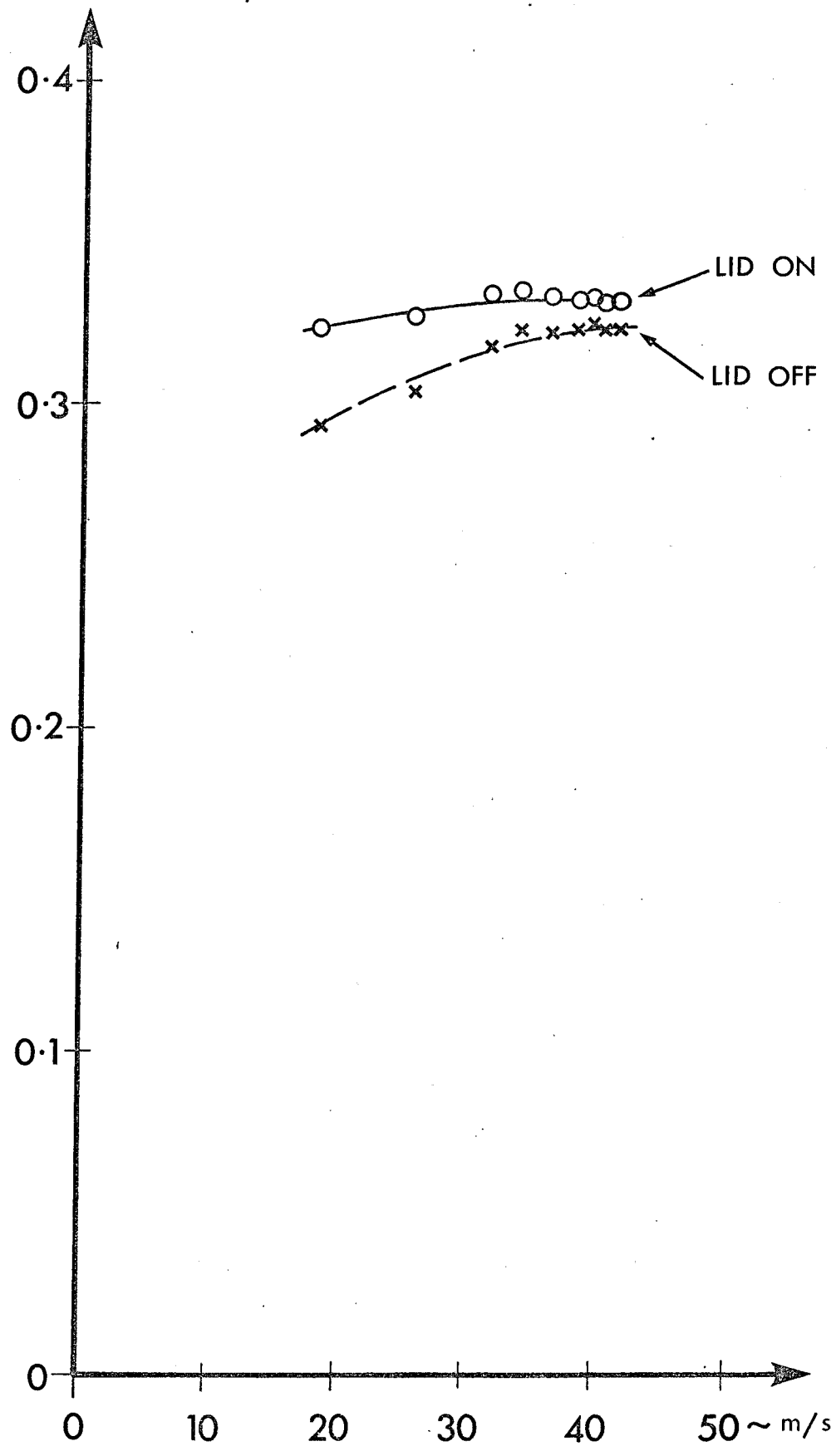

Fig. 9

$C_L \sim \alpha$

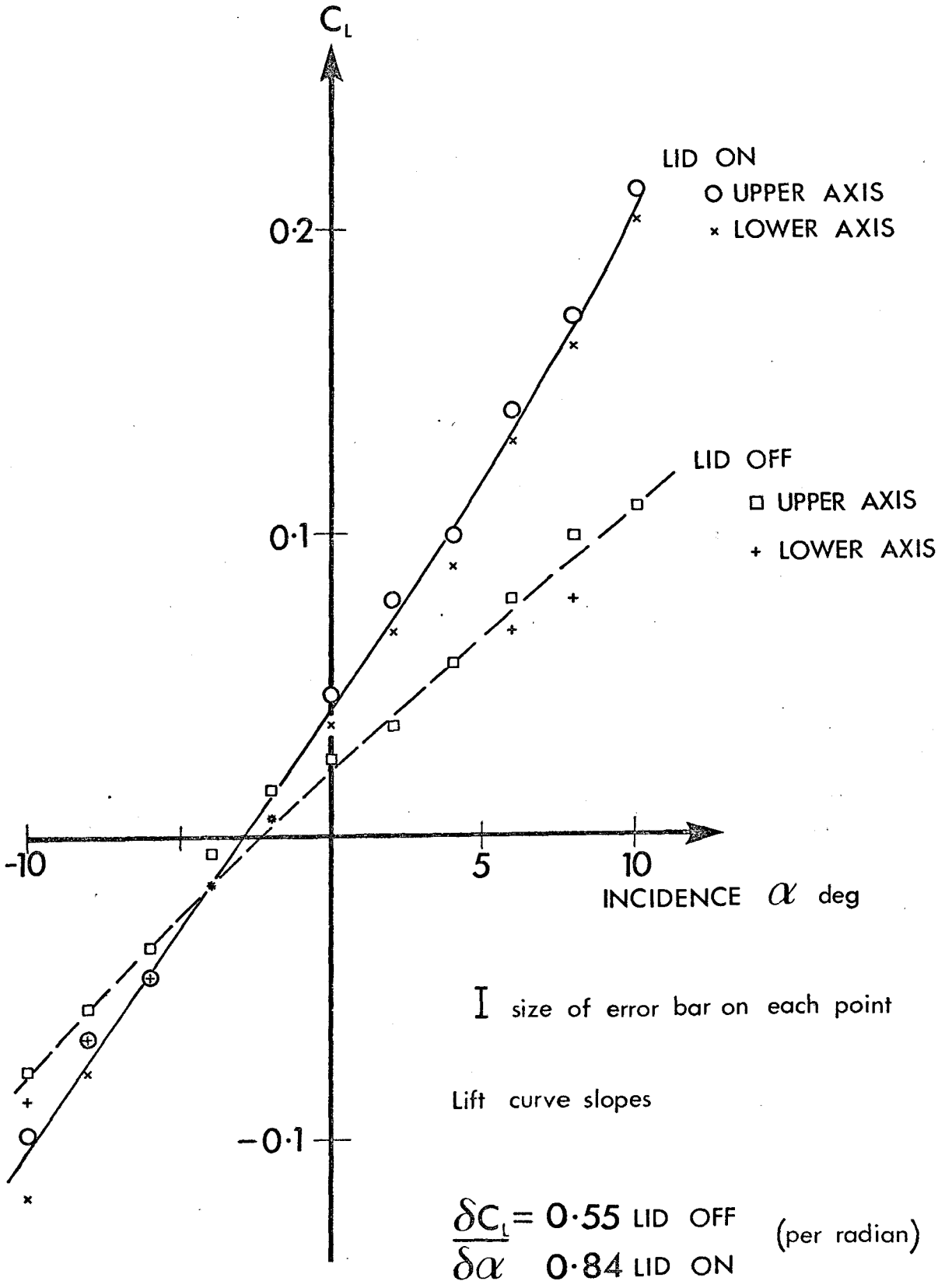

I size of error bar on each point

Lift curve slopes

$\frac{\delta C_L}{\delta \alpha}$ = 0·55 LID OFF
0·84 LID ON
(per radian)

Fig. 10

$C_D \sim \alpha$

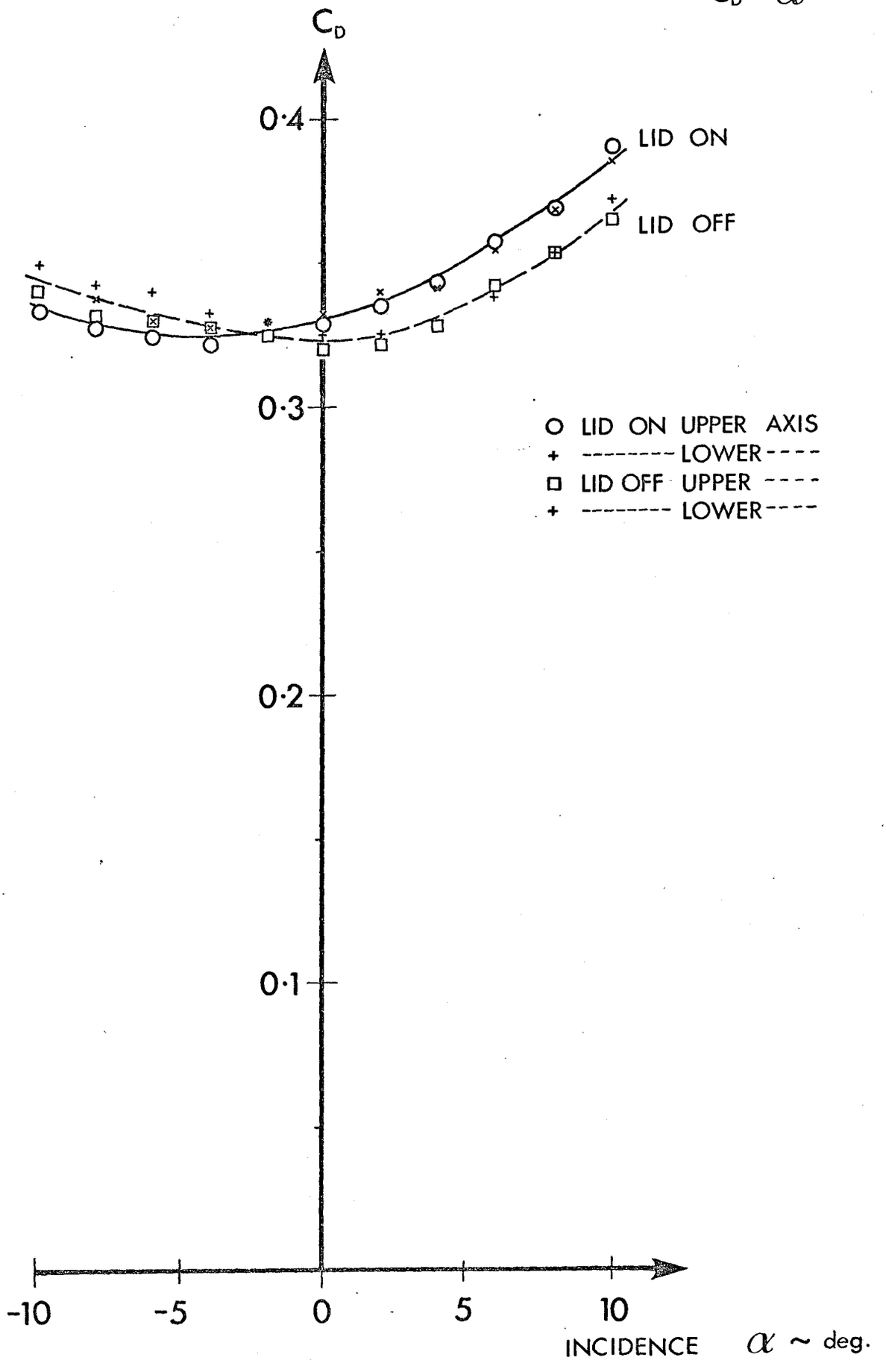

Fig. 11

$C_M \sim \alpha$

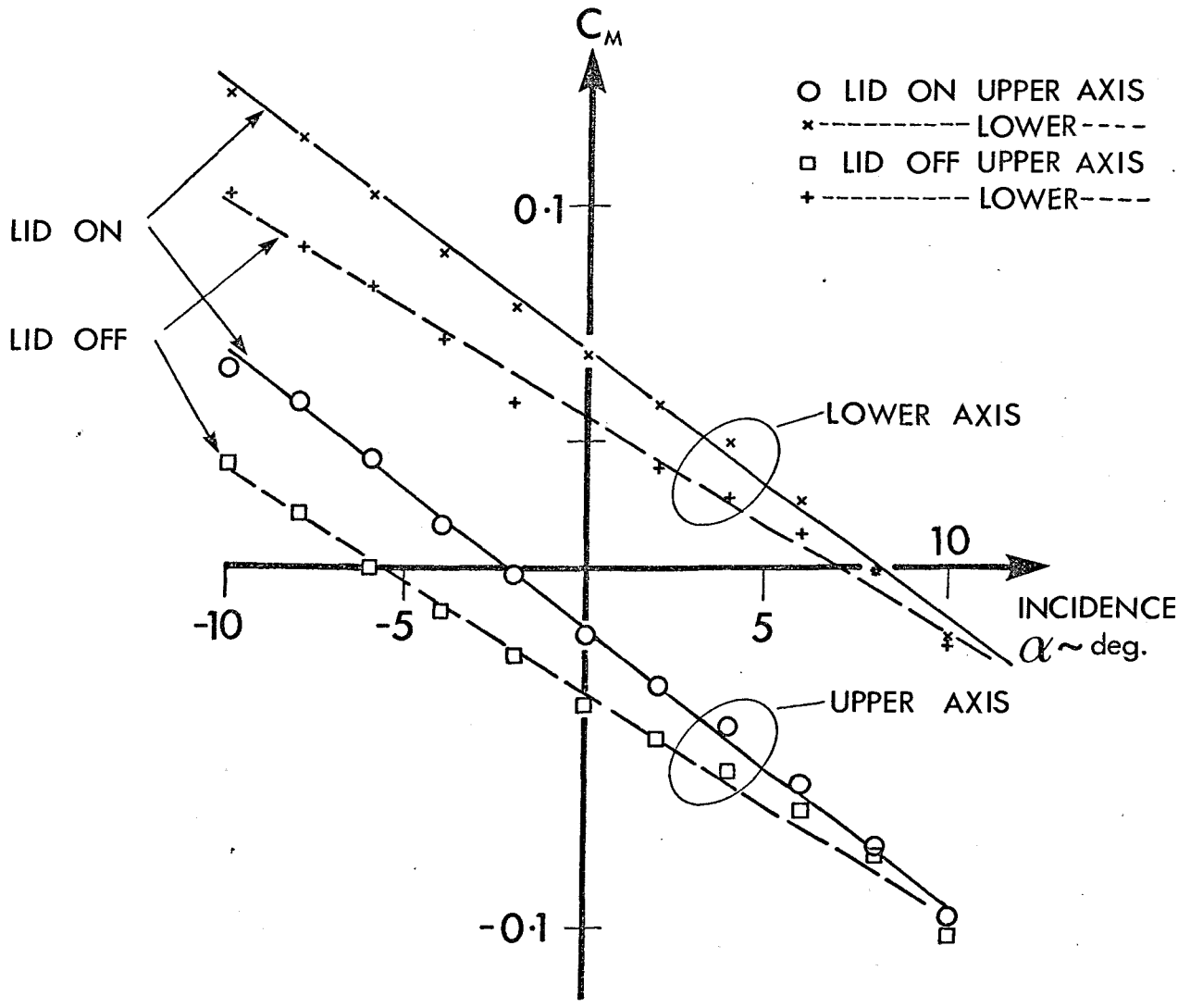

Fig. 12

$C_M \sim C_L$

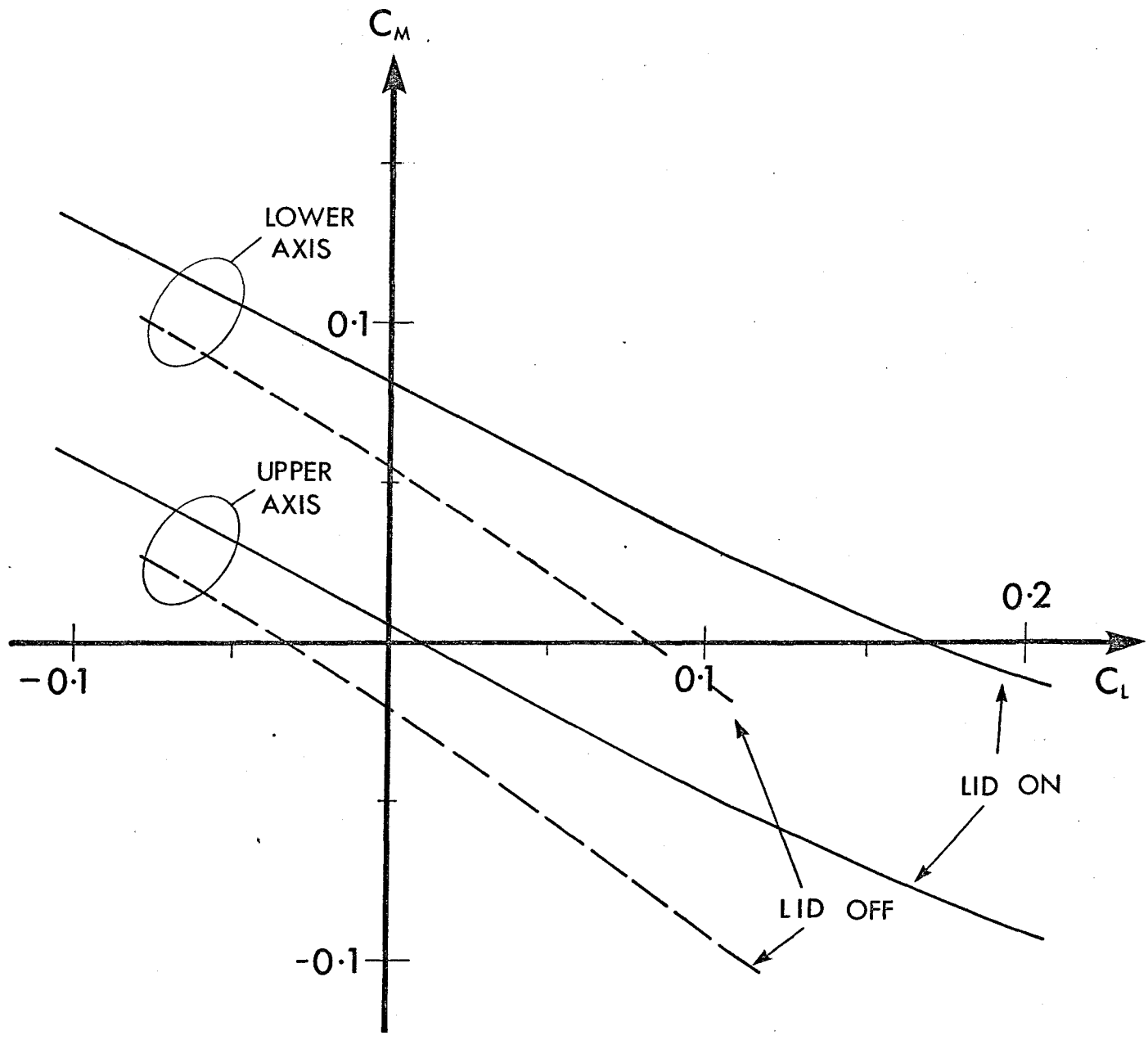

Fig. 13

$C_Y \sim \psi$

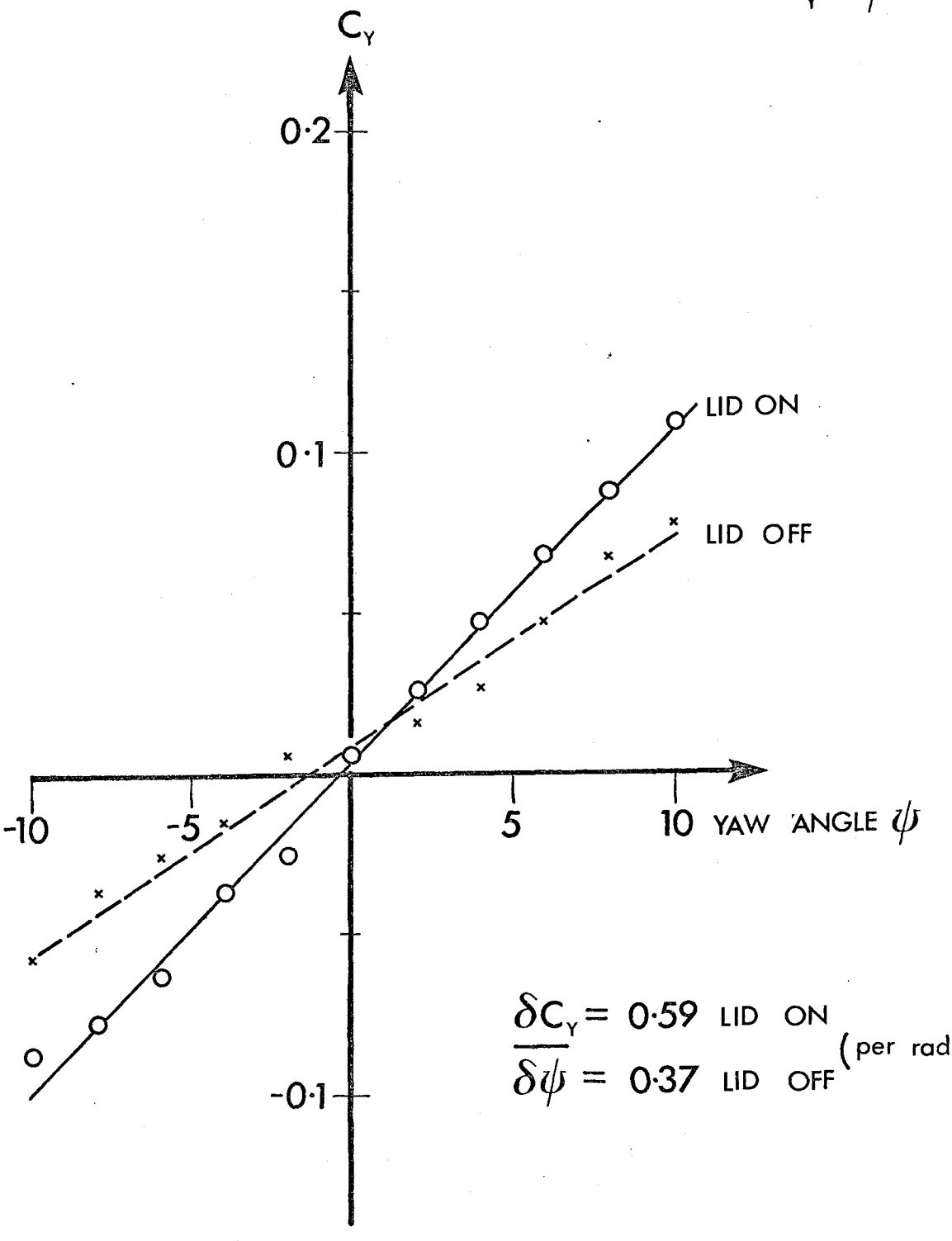

$\frac{\delta C_Y}{\delta \psi}$ = 0·59 LID ON
= 0·37 LID OFF (per radian)

Fig. 14

$C_D \sim \psi$

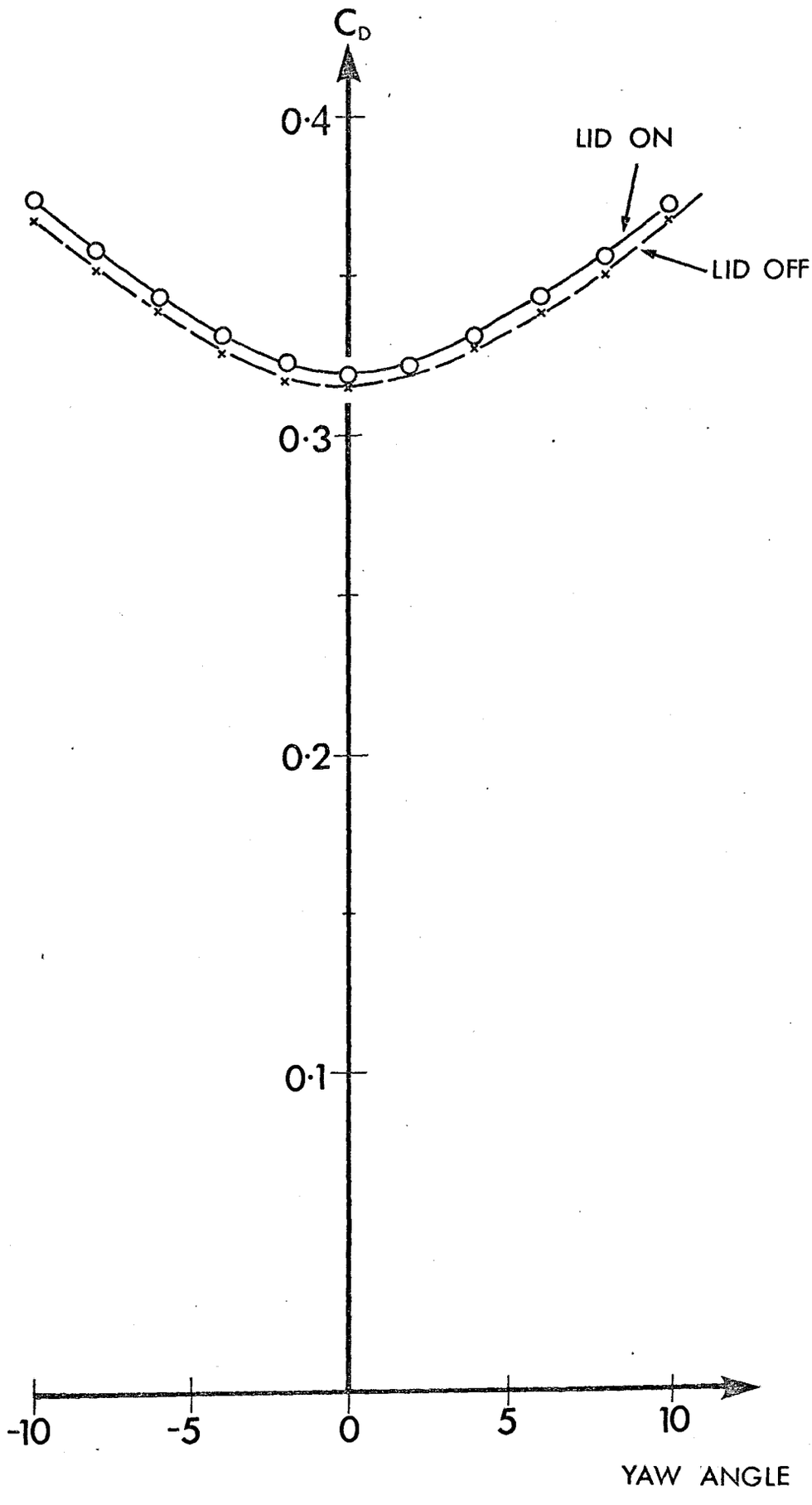

Fig. 15

$C_N \sim \psi$

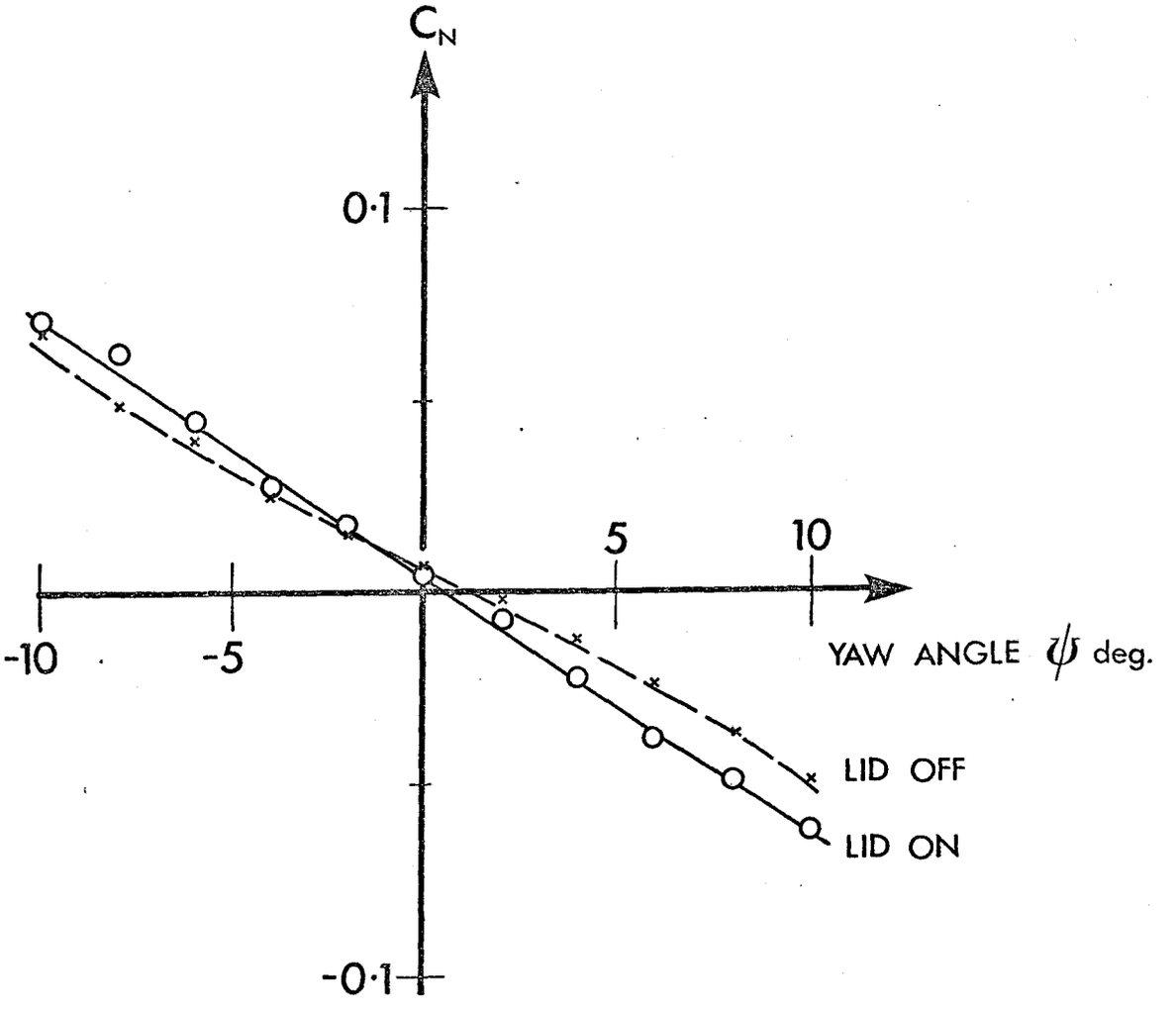

Fig. 16

$C_N \sim C_Y$

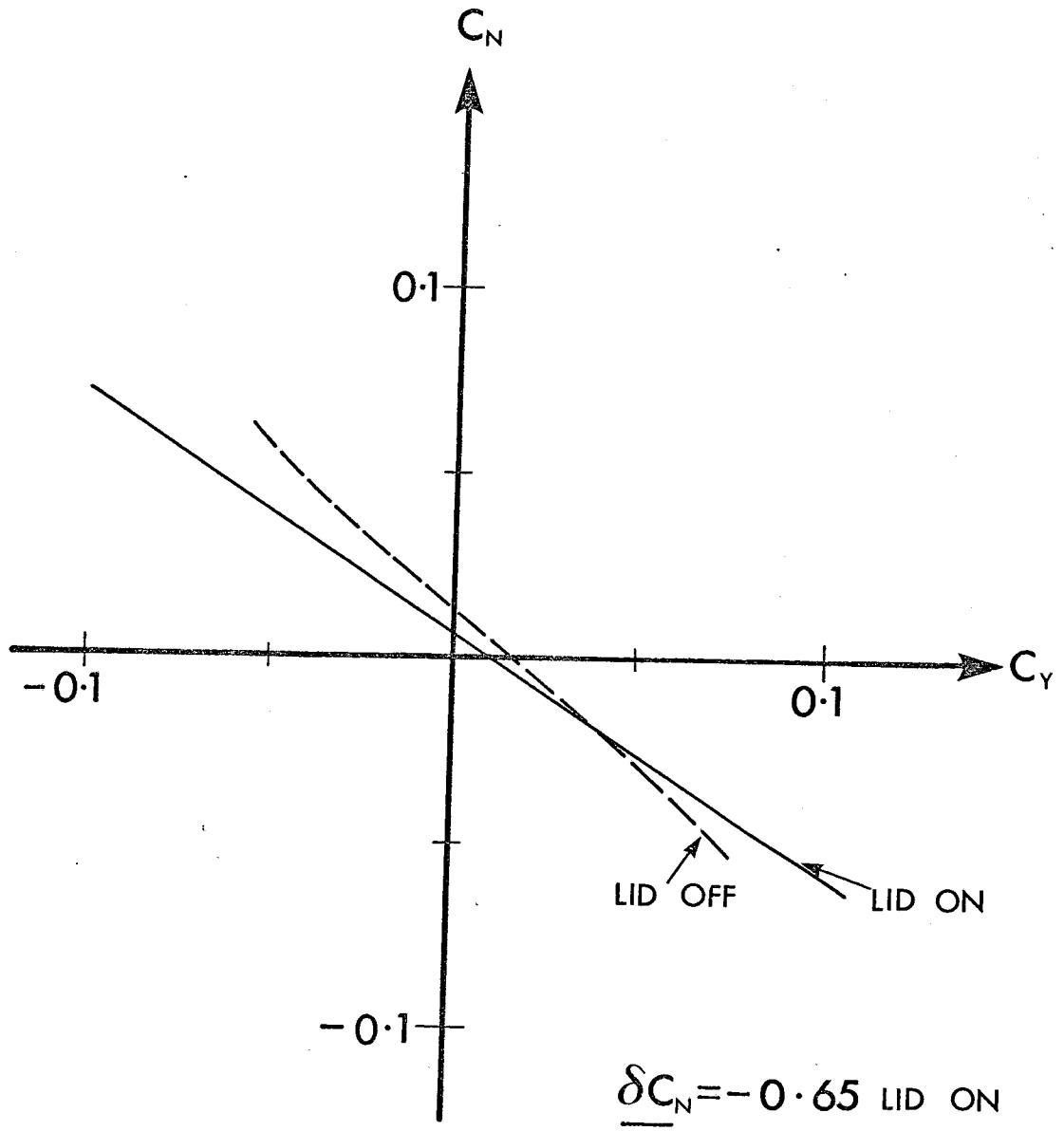

$\frac{\delta C_N}{\delta C_Y} = \frac{-0.65}{-0.85}$ LID ON / LID OFF

in the range $-2° \leqslant \psi \leqslant 2°$

FIG. 17 RANGE OF TOW POINT LOCATIONS RELATIVE TO THE FRONT FRAME